



Dosimetric comparison between stereotactic body radiotherapy and carbon-ion radiation therapy for prostate cancer

He-Fa Huang^{1,2}, Xing-Xin Gao¹, Qiang Li³, Xiao-Yun Ma⁴, Lan-Ning Du⁵, Peng-Fei Sun⁶, Sha Li¹

¹Department of Irradiation Oncology, the 940th Hospital of Joint Logistics Support Force of Chinese People's Liberation Army, Lanzhou, China; ²School of Nuclear Science and Technology, Lanzhou University, Lanzhou, China; ³Institute of Modern Physics, Chinese Academy of Sciences, Lanzhou, China; ⁴Heavy Ion Center, Wuwei Cancer Hospital, Wuwei, China; ⁵Department of Radiotherapy, The First Hospital of Lanzhou University, Lanzhou, China; ⁶Department of Radiotherapy, The Second Hospital of Lanzhou University, Lanzhou, China

Contributions: (I) Conception and design: S Li, XX Gao; (II) Administrative support: S Li; (III) Provision of study materials or patients: None; (IV) Collection and assembly of data: PF Sun, LN Du; (V) Data analysis and interpretation: Q Li, XY Ma; (VI) Manuscript writing: All authors; (VII) Final approval of manuscript: All authors.

Correspondence to: Sha Li, MM. Department of Irradiation Oncology, the 940th Hospital of Joint Logistics Support Force of Chinese People's Liberation Army, 333 Nanbinhe Road, Lanzhou 730050, China. Email: lishalsn@126.com.

Background: Prostate cancer rates have been steadily increasing in recent years. As high-precision radiation therapy methods, stereotactic body radiation therapy (SBRT) and carbon-ion radiation therapy (CIRT) have unique advantages. Analyzing the dosimetric differences between SBRT and CIRT in the treatment of localized prostate cancer can help provide patients with more accurate, individualized treatment plans.

Methods: We selected computed tomography positioning images and the contours of target volumes of 16 patients with localized prostate cancer who received radiotherapy. We delineated the organs at risk (OARs) on the CyberKnife (CK) treatment planning system (TPS) MultiPlan4.0, which were imported into the CIRT uniform scanning TPS HIMM-1 ci-Plan. Two treatment plans, SBRT and CIRT, were designed for the same patient, and we used SPSS 22.0 for the statistical analysis of data.

Results: Both SBRT and CIRT plans met the prescribed dose requirements. In terms of target volume exposure dose, D2 ($P<0.001$), D5 ($P<0.001$), D50 ($P<0.001$), D90 ($P=0.029$), D95 ($P<0.001$), D98 ($P<0.001$), and D_{mean} ($P<0.001$) under SBRT were significantly higher than those under CIRT; the conformity index (CI) under SBRT was significantly better than that under CIRT ($P<0.001$); the target volume coverage rate (V95%) and dose homogeneity index (HI) under CIRT were significantly better than those under SBRT ($P<0.001$). In terms of OAR exposure dosage, the D_{max} of the bladder and rectum under SBRT was significantly lower than that under CIRT ($P<0.001$), but D_{mean} was in the other direction; the exposure dose of the intestinal tract under CIRT was significantly lower than that under SBRT ($P<0.05$); D_{max} of the femoral head under CIRT was significantly lower than that under SBRT ($P<0.05$), and there was no statistical difference between them at other doses.

Conclusions: In this study, we found that when CIRT was used for treating localized prostate cancer, the dose distribution in target volume was more homogeneous and the coverage rate was higher; the average dose of OARs was lower. SBRT had a better CI and higher dose in target volume; the dose hotspot was lower in OARs. It is important to comprehensively consider the dose relationship between local tumor and surrounding tissues when selecting treatment plans.

Keywords: Carbon-ion radiation therapy (CIRT); dosimetry; localized prostate cancer; stereotactic body radiotherapy (SBRT)

Submitted Mar 17, 2023. Accepted for publication Aug 25, 2023. Published online Sep 22, 2023.

doi: 10.21037/qims-23-340

View this article at: <https://dx.doi.org/10.21037/qims-23-340>

Introduction

Prostate cancer, a common malignant tumor in the male urogenital system that occurs in the prostatic epithelium, is a major public health issue (1,2). With advances in the development of prostate-specific antigen (PSA) screening, prostate-specific membrane antigen (PSMA), genetic testing, molecular imaging, and other technologies (3-6), the incidence rate of prostate cancer is increasing year by year, as shown in *Table 1* (7,8).

Localized prostate cancer is a chronic disease and is not life-threatening in the short term. An effective mode of treatment can improve the quality of life of patients while improving their survival rate and reducing toxicity and side effects (9). As one of the radical treatments for localized prostate cancer, radiotherapy is not significantly different from surgery in terms of tumor control rate, survival rate, and incidence of toxicity and side effects (10-12), while it has the advantages of broad indications, fewer complications, good curative effect, and is accepted by most patients (13,14).

At present, most stereotactic body radiotherapy (SBRT) is done on the CyberKnife (CK) (15). It integrates real-time image guidance and dynamic tumor tracking technology, and has the advantages of short treatment time, high conformity index (CI) of target volume, high dose gradient, high treatment accuracy, low toxicity and side effects, and high local control (LC) rate (16,17), and is one of the latest and most advanced photon radiotherapy equipment.

The $^{12}\text{C}^{6+}$ beam used in carbon-ion radiation therapy (CIRT) has high linear energy transfer (LET), and its relative biological effect is about 2.5–3 times that of X-ray. The reversed dose distribution and spread-out Bragg peak (SOBP) enable it to release a large amount of energy in the target volume, which can achieve targeted tumor killing (18,19).

When compared with conventional radiotherapy (X-ray and γ -ray), both SBRT and CIRT have the advantages of high single dose, less fractions, and good protection of normal tissues. It was found that, on the premise of ensuring the efficacy and quality of life, increasing the single dose can reduce the total dose required (20). In this paper, we aimed to preliminarily explore the dosimetric advantages and heterogeneity of SBRT and CIRT, and provide theoretical and evidence support for clinicians, physicists, and patients to select the treatment methods.

Methods

Clinical data

In strict accordance with the inclusion criteria for the retrospective study, we included the positioning images [computed tomography (CT)] of 16 patients with localized prostate cancer who sought medical treatment at the Department of Radiotherapy of the 940th Hospital of Joint Logistics Support Force of Chinese People's Liberation Army, the Department of Radiotherapy of the First Hospital of Lanzhou University, and the Department of Radiotherapy of Lanzhou University Second Hospital from March 2014 to April 2021 (12 cases, 2 cases, and 2 cases, respectively). The pathology diagnosis was confirmed using prostate needle biopsy. In terms of case selection, we identified patients suitable for SBRT and CIRT treatments. Among the 16 patients, not all of them had been treated with CK and CIRT, and for this study, we considered patients who would be suitable for these two treatments. A clinician approved by the Chief Physician was responsible for outlining of the tissue for all cases in the study.

The main clinical symptoms were progressive dysuria, frequent urination, urgency of urination, increased nocturia, and even urinary incontinence. The average age was 73 years (43–89 years), and the average size of the primary tumor was 62.91 mm (47.57–90.84 mm). According to the guidelines of the National Comprehensive Cancer Network (NCCN), there were 5, 6, and 5 patients with low-, medium-, and high-risk of localization, respectively. In this retrospective study, all the positioning images were of treatment-naive patients. Lymph node or distant metastasis was excluded, and there was no contraindication to radiotherapy. This study was conducted in accordance with the Declaration of Helsinki (as revised in 2013). The study was approved by the Ethics Committee of the 940th Hospital of Joint Logistics Support Force of Chinese People's Liberation (No. 2022KYLL074). Written informed consent was obtained from all participants.

The new senior engineer of Gao Bank developed the CK treatment plan in this study, and engineer Ma XY drew up the CIRT treatment plan. Both of these professionals have more than 10 years of relevant work experience. Chief Physician Li was responsible for the review.

Position fixation and CT scan

Before positioning and scanning, a special vacuum negative

Table 1 Statistics of morbidity and mortality of prostate cancer in China

Year	Incidence rate			Mortality rate		
	No. of new cases (10 ⁴)	% of all men in China	Rank	No. of death cases (10 ⁴)	% of all men in China	Rank
2013 (7)	5.98	2.9	6	2.52	1.8	10
2020 (8)	11.5	4.7	6	5.1	2.8	7

pressure pad or thermoplastic phantom was made for patients. All patients were placed in a naturally relaxed supine position, with their hands crossed, holding their elbows and placed above the forehead, and their lower limbs naturally flat. Positron emission tomography/computed tomography (PET-CT) simulated positioner (Siemens, Germany), CT simulated positioner, and MRI were used for positioning and scanning. The scanning range was from the upper edge of the lumbar vertebra 3 to 5 cm below the ischial tubercle. The layer thickness and layer spacing of CT scanning were both 2–5 mm. The positioning images were uploaded to the CK MultiPlan4.0 treatment planning system (TPS) workstation in medical digital image and Digital Imaging and Communications in Medicine (DICOM) format to delineate the contours of target volume and organs at risk (OARs).

Target volume delineation and prescribed dose

In accordance with the International Commission on Radiation Units and Measurements (ICRU) Report 83 (21), we delineated the target volume and OARs using the CK MultiPlan 4.0 TPS workstation, and the delineated tissue contours were imported into the CIRT TPS ci-Plan. As CT and MRI could not accurately detect all foci in the prostate (22), the gross tumor volume (GTV) was usually not delineated.

After CT image reconstruction, the clinical target volume (CTV), planning target volume (PTV), and OARs were directly delineated. The CTV of localized low-risk patients included the whole prostate, and the CTV of medium- and high-risk patients included the prostate and 1–2.5 mm proximal end of the external seminal vesicle gland (23). To eliminate the uncertainties caused by organ movement, positioning errors, and dose distribution, PTV was expanded outward on the basis of CTV. As the prostate is close to the rectum, PTV was expanded outward by 3 mm along the direction of rectum, and expanded outward uniformly by 5 mm along the other directions (24). Manual correction was performed according to individual differences.

According to the target volume delineation principles of the OARs in the Radiation Therapy Oncology Group

(RTOG) (25), we included the rectum, bladder, intestinal tract, and femoral heads in the delineation range of OARs (26,27). The rectum was delineated horizontally from the ischial tubercle to the junction of rectum and sigmoid colon. The whole bladder was delineated. The delineated intestinal tract included the corresponding layer of PTV and all small intestine and colon (including intestinal walls and contents), and the delineated femoral heads included femoral heads and femoral neck structures on both sides.

In this study, we designed two different treatment plans for the same patient with the biological equivalent dose (BED) of 161.28 Gy/Gy [relative biological effectiveness (RBE)]. The prescribed doses of SBRT and CIRT were 35.47 Gy/5f and 57.6 Gy (RBE)/16f, respectively (28). Based on $E = \alpha D + \beta D^2 = (\alpha)(nd) \left[1 + d/(\alpha/\beta) \right]$, we deduced that

$$BED = E/\alpha = nd \left[1 + d/(\alpha/\beta) \right] = D_1 \left(1 + \frac{d_1}{\alpha/\beta} \right) = D_2 \left(1 + \frac{d_2}{\alpha/\beta} \right),$$

$$n_1 d_1 (d_1 + \alpha/\beta) = n_2 d_2 (d_2 + \alpha/\beta) \text{ where } D \text{ represents the total dose of radiotherapy; } d \text{ represents fractional dose; } n \text{ indicates the count.}$$

We obtained the prescription doses of SBRT and CIRT by combining the clinically effective prescription doses. However, the use of this method also has some limitations, for example, in the case of identical BEDs, both need to meet the requirements of clinical use.

Through a literature review, we identified that the most commonly used CK segmentation methods are 35–36.25 Gy/5f, and the most commonly used CIRT is 57.6 Gy (RBE)/16f for radiotherapy in prostate cancer. As our study was based on clinical use, we used the CIRT BED as the reference. We additionally determined the prescription dose and segmentation method of CK to analyze the heterogeneity of their dosimetric distribution. As $BED = E/\alpha = nd \left[1 + d/(\alpha/\beta) \right] = D_1 \left(1 + \frac{d_1}{\alpha/\beta} \right) = D_2 \left(1 + \frac{d_2}{\alpha/\beta} \right)$, in order to facilitate comparative analysis of the differences between the two during data processing, we analyzed equivalent doses in 2 Gy/f (EQD₂), which was converted into 2 Gy/f for conventional radiotherapy, and we did

Table 2 Dose limits of normal tissues under SBRT and CIRT for the treatment of prostate cancer

Organ	SBRT-CK (5 frequency)			CIRT (16 frequency)
	Volume (cm ³)	Dose (Gy)	D _{max} (Gy)	Volume dose [Gy (RBE)]
Bladder	<15	18.3	38	D50%≤50
Rectum	<20	25	38	D40%≤50, D20%≤60
Bowel	<5	19.5	35	D50%≤30, D _{max} ≤45–50
Femoral heads	<10	30	–	D5%≤50, D15%≤30

SBRT-CK (5 frequency): for bladder, the volume with a dose of 18.3 Gy should not exceed 15 cm³, and the D_{max} should not exceed 38 Gy; CIRT (16 frequency): bladder D50%, the exposure dose of 50% bladder volume should not exceed 50 Gy (RBE). SBRT-CK: in SBRT radiotherapy, the device used is the Cyberknife CK. SBRT, stereotactic body radiotherapy; CIRT, carbon-ion radiation therapy; CK, CyberKnife; RBE, relative biological effectiveness; D_{max}, maximum irradiation dose.

not use BED. Since the volume covered by 95% of the prescription dose cannot be calculated in CK, we used the CI algorithm of the CK system TPS in SBRT, namely: $CI = \frac{PIV}{TIV}$. In statistics, for intuitive analysis, it is converted to a value less than 1.

Plan design

We formulated the SBRT plan in the CK MultiPlan4.0 TPS (CyberKnife, Accuray Inc. Sunnyvale, CA, USA). We adopted the reverse design principle and 6 MV X-ray energy and used the gold mark/spine tracking method. The positioning center was the geometric center of the tumor, the size of the applicator was about 2nd/3rd of the maximum diameter of the tumor (29), the dose rate was 800 MU/min, and 95% PTV was required to receive at least 95% of the prescribed dose. As per the RTOG standard (30), the dose limits of normal tissues are shown in *Table 2*. The parameters were optimized and evaluated according to the isodose curves and dose-volume histogram (DVH) diagrams while ensuring the coverage of the target volume.

In the CIRT plan (HIMM-1ci-Plan), we adopted the forward design principle and dual-field interpenetrating irradiation. The single Bragg peak is sharp and narrow—in order to be suitable for the treatment of tumors of different sizes, Bragg needs to be appropriately spread out. In this study, we used uniform scanning technology for carbon ion treatment as per the Treatment Room 2 of the Heavy-Ion Medical Machine (HIMM) facility in Wuwei to scan the beam into wide beam. The beam was horizontally expanded with triangular wave and other scanning methods, the Bragg peak of the beam was longitudinally widened using the ridge filter, and we used the multi-leaf collimator (MLC) for conformal irradiation of the maximum cross section.

As per the RTOG standards, 95% isodose lines should cover 100% PTV (27); the dose limits of normal tissues are shown in *Table 2*. The dose drops steepness at the rear edge of the ¹²C⁶⁺ beam field was better than that at the side edge. When the PTV dose conditions were met, the exposure dose of OARs in the adjacent target volume was reduced as far as possible to meet the clinical treatment requirements (31).

Plan evaluation

Based on the recommendations of the RTOG guidelines (25) and the ICRU Report 83 (21), we evaluated the treatment plan from the perspective of the dose distribution of the target volume, the CI, the homogeneity index (HI), and the dose distribution of OARs. The dosimetric parameters of SBRT and CIRT cannot be directly compared in radiobiology and need to be converted into EQD₂ according to the linear-quadratic (L-Q) model; this is also applicable to CIRT (32). The α/β value of the tumor target volume was 1.5 Gy (33,34), that is, 5 Gy for the rectum, 10 Gy for the bladder, and 8 Gy for the intestinal tract (35).

Evaluation of PTV dosimetric parameters

We conducted a comprehensive plan evaluation based on the isodose curves and DVH diagrams. According to the ICRU Report 83, the maximum exposure dose of the target volume is D₂, the minimum exposure dose is D₉₈, the average exposure dose is expressed in D_{mean}, and D₉₅ is used to evaluate the coverage of the target volume dose. In this study, we used D₉₈, D₉₅, D₉₀, D₅₀, D₅, D₂, D_{mean}, CI, and HI to evaluate the dose distribution of PTV, where D₂ represents the minimum exposure dose received by 2% volume.

CI: the CI of PTV in CIRT is shown in Formula [1], where PTV₉₅ represents 95% of the PTV volume, PTV

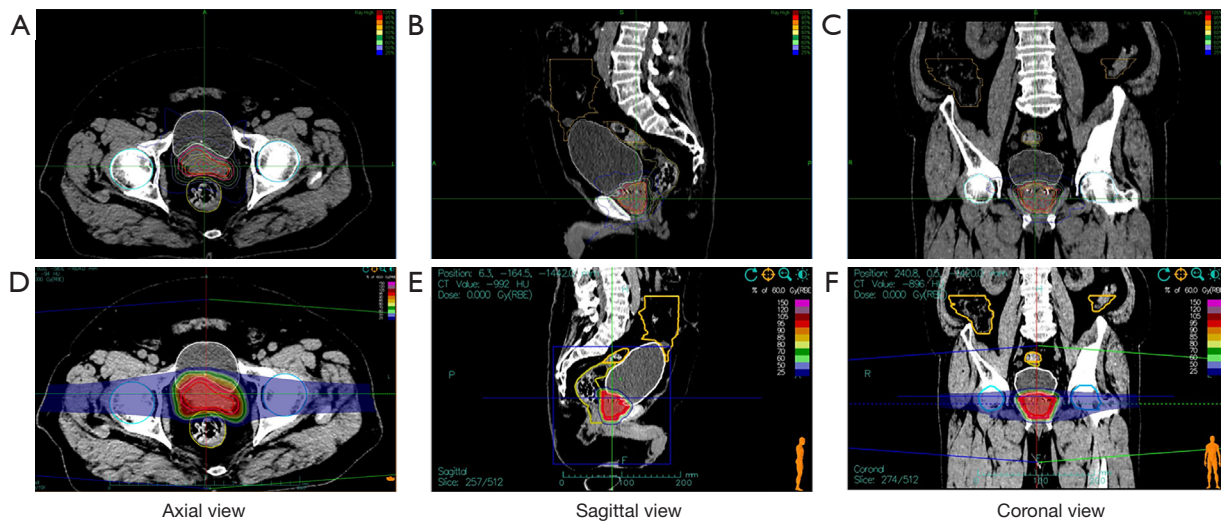


Figure 1 Isodose curves of two TPSs for a patient (A-C: SBRT, D-F: CIRT). TPS, treatment planning system; SBRT, stereotactic body radiotherapy; CIRT, carbon-ion radiation therapy.

represents the volume of PTV, and V95 represents the volume covered by 95% of the prescribed dose. The CI of the PTV of CK is shown in Eq. [2], where PIV represents the volume of all tissues wrapped by the prescribed dose, and TIV represents the target volume wrapped by the prescribed dose. CI can objectively reflect the conformity of radiotherapy dose distribution to the size and shape of the target volume. When CI is closer to 1, it means higher conformity and better dose distribution (21,36). The CI of CK is normalized.

$$CI = \frac{(PTV95)^2}{PIV \cdot V95} \tag{1}$$

$$CI = \frac{PIV}{TIV} \tag{2}$$

The HI, which can be used to analyze and quantify the homogeneity of dose distribution in the target volume, is shown in Eq. [3]. When HI is closer to 0, it means more homogeneous dose distribution in the target volume.

$$HI = \frac{D2 - D98}{D_{mean}} \tag{3}$$

Evaluation parameters of OARs

- ❖ Bladder: D_{max} , D_{mean} , D50;
- ❖ Intestinal tract: D_{max} , D_{mean} , D50;
- ❖ Rectum: D_{max} , D_{mean} , D40, D20;
- ❖ Bilateral femoral heads: D_{max} , D_{mean} , D15, D5.

Statistical analysis

We used IBM SPSS 22.0 software for the statistical analysis of all data in this study, and the data are expressed as mean ± standard deviation ($\bar{x} \pm s$). The volume dose parameters of PTV and OARs were collected according to the DVH diagrams. The samples in normal distribution were tested using paired-samples *t*-test; the samples not in normal distribution were tested using paired-samples rank sum test. The difference was statistically significant when $P < 0.05$.

Results

In this study, we formulated a total of 32 treatment plans for 16 patients with localized prostate cancer. We performed the dosimetric analysis on the target volumes and OARs, and all doses were converted into EQD₂. In the CK treatment plan, 3 cases still failed to cover 95% PTV volume (87.12–92.82%) with 95% prescribed dose, while CIRT could cover 100% PTV volume with 95% prescribed dose. The transverse, sagittal, and coronal dose distribution of SBRT and CIRT of one case are shown in *Figure 1*, and DVH of one case is shown in *Figure 2*.

Dosimetric analysis of PTV

The PTV related parameters of the two treatment plans are shown in *Table 3*. In this study, the volume percentages covered by 95% prescribed dose of the PTVs of SBRT

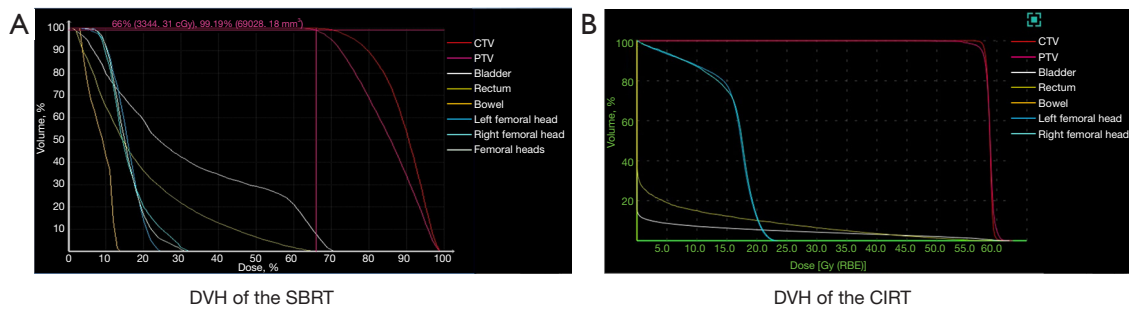


Figure 2 DVH diagram of two TPSs for a patient (A: SBRT, B: CIRT). CTV, clinical target volume; PTV, planning target volume; DVH, dose-volume histogram; SBRT, stereotactic body radiotherapy; CIRT, carbon-ion radiation therapy; TPS, treatment planning system.

Table 3 Comparison of dose distribution in target volumes between SBRT and CIRT treatment plans

Organ	Volume dose	SBRT (Gy)	CIRT [Gy (RBE)]	t	P
PTV	D2	146.75±1.87	89.53±2.79	-82.480	<0.001
	D5	144.01±2.51	88.06±2.37	-75.639	<0.001
	D50	112.61±6.05	84.98±1.84	-16.428	<0.001
	D90	78.13±7.49	82.60±0.88	2.423	0.029
	D95	69.93±9.21	80.64±0.00	4.654	<0.001
	D98	62.29±10.90	76.71±1.81	5.146	<0.001
	D _{mean}	109.31±4.89	84.77±1.48	-19.663	<0.001
	V95%	0.93±0.04	1.00±0.00	6.336	<0.001
	CI	0.89±0.04	0.81±0.04	-5.1	<0.001
	HI	0.45±0.08	0.09±0.03	-15.601	<0.001

Data are expressed as mean ± standard deviation ($\bar{x} \pm s$), and 2 is retained as a decimal. D98 represents the minimum exposure dose of PTV; D2 represents the maximum exposure dose of PTV; V95% represents the volume percentage of PTV covered by 95% prescribed dose, and SBRT CI is normalized. PTV, planning target volume; SBRT, stereotactic body radiotherapy; CIRT, carbon-ion radiation therapy; RBE, relative biological effectiveness; CI, conformity index; HI, homogeneity index.

and CIRT were 93.24±4.00 and 100±0.00, respectively ($P < 0.001$); HI was 0.45±0.08 and 0.09±0.03, respectively ($P < 0.001$); CI was 0.89±0.04 and 0.81±0.04, respectively after normalization ($P < 0.001$); D98 was 62.29±10.90 and 76.71±1.81, respectively ($P < 0.001$); D95 was 69.93±9.21 and 80.64±0.00, respectively ($P = 0.029$); D90 was 78.13±7.49 and 82.60±0.88, respectively ($P < 0.001$); D50 was 112.61±6.05 and 84.98±1.84, respectively ($P < 0.001$); D5 was 144.01±1.87 and 88.06±2.37, respectively ($P < 0.001$); D2 was 146.75±1.87 and 89.53±2.79, respectively ($P < 0.001$), and D_{mean} was 109.31±4.89 and 84.77±1.48, respectively ($P < 0.001$), which all had significant clinical implication.

When PTV dose volume was more than 90%, the target volume dose of CIRT was significantly higher than that of

SBRT, and this was the opposite when PTV dose volume was less than 90%. With respect to the SBRT target volume, the overall dose was higher, the CI was closer to 1, and the conformity was better. With respect to the CIRT target volume, the coverage was better, the HI was closer to 0, and dose distribution was more homogeneous. Details are given in *Table 3* and *Figure 3*. One of the advantages of SBRT is the rapid dose drop. The hemispherical beam distribution in CK disperses the dose such that a high dosage is concentrated in the target area while the dosage in the surrounding normal tissue is low, resulting in a large dose gradient. Uniform dose distribution is also a requirement of using CIRT, and the presence of the Bragg peak in CIRT flattens the dose distribution in the tumor target area.

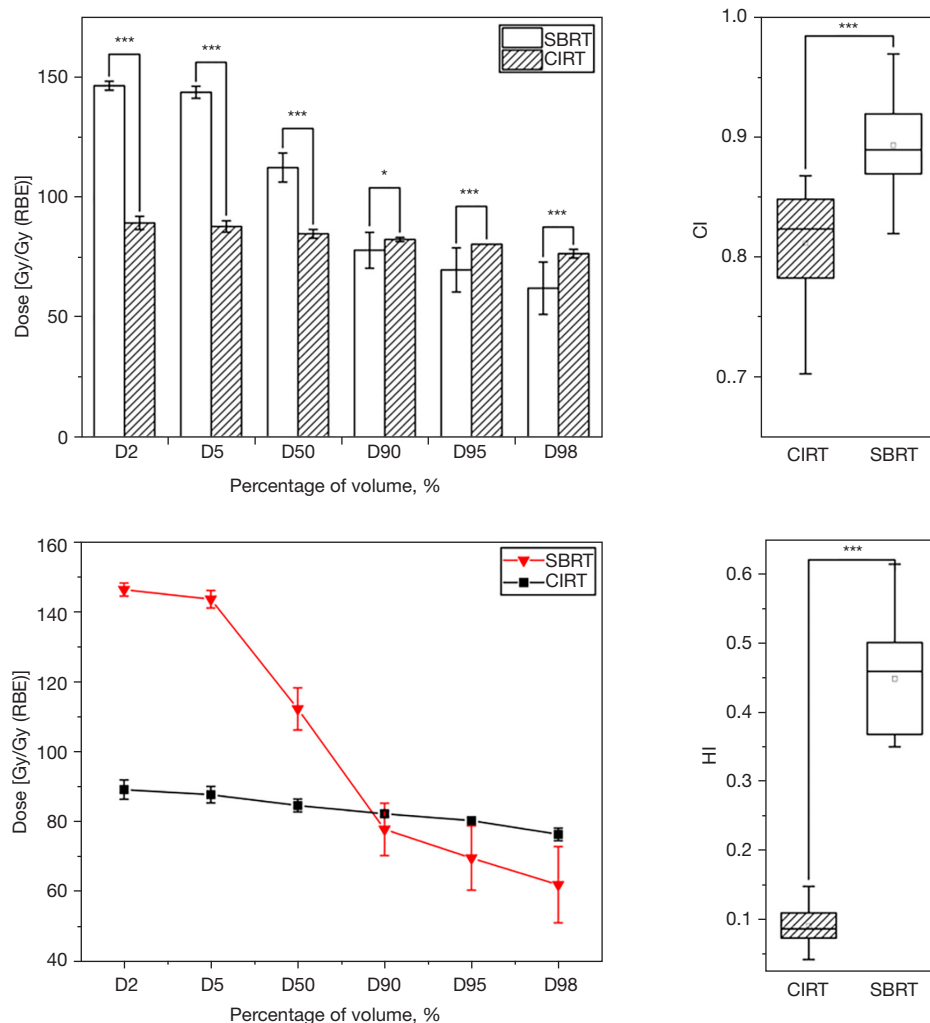


Figure 3 PTV volume dose histogram, line chart, and CI and HI box plots of 16 patients. *, $P < 0.05$, ***, $P < 0.001$. RBE, relative biological effectiveness; SBRT, stereotactic body radiotherapy; CIRT, carbon-ion radiation therapy; PTV, planning target volume; CI, conformity index; HI, homogeneity index.

Analysis of dosimetric parameters of OARs

Exposure dose of bladder

The D_{max} (maximum exposure dose) of SBRT and CIRT was 46.52 ± 5.90 and 70.04 ± 2.69 ($P < 0.001$), D_{mean} (average exposure dose) was 12.64 ± 3.97 and 4.45 ± 2.77 ($P < 0.001$), and $D50$ was 11.16 ± 3.60 and 0.13 ± 0.31 ($P < 0.001$), respectively, all of which had significant differences. The relevant parameters are shown in *Table 4* and *Figure 4*. There were individual hotspots in the bladder in the CIRT treatment plan, resulting in the D_{max} being significantly greater than that in SBRT; the D_{mean} and $D50$ of CIRT were significantly lower than those of SBRT, so the overall exposure dose of

the bladder was lower.

Exposure dose of intestinal tract

The D_{max} of SBRT and CIRT was 20.65 ± 12.52 and 10.81 ± 22.96 ($P = 0.008$), D_{mean} was 4.43 ± 2.18 and 0.06 ± 0.21 ($P < 0.001$), and $D50$ was 4.33 ± 2.24 and 0.00 ± 0.00 ($P < 0.001$), respectively, all of which had significant differences. The relevant parameters are shown in *Table 4* and *Figure 4*. The exposure dose of intestinal tract of CIRT was significantly lower than that of SBRT, and the average dose was basically close to 0 Gy (RBE), which realized better intestinal protection. Two patients had large tumor target volume, which was partially surrounded by the intestine, resulting in

Table 4 Comparison of dose distribution in OARs between SBRT and CIRT treatment plans

Organ	Volume dose	SBRT (Gy)	CIRT [Gy (RBE)]	<i>t</i>	P
Bladder	D _{max}	46.52±5.90	70.04±2.69	20.732	<0.001
	D _{mean}	12.64±3.97	4.45±2.77	-9.479	<0.001
	D50	11.16±3.60	0.13±0.31	12.888	<0.001
Bowel	D _{max}	20.65±12.52	10.81±22.96	3.032	0.008
	D _{mean}	4.43±2.18	0.06±0.21	8.393	<0.001
	D50	4.33±2.24	0.00±0.00	7.745	<0.001
Rectum	D _{max}	60.69±5.31	70.76±6.51	7.021	<0.001
	D _{mean}	13.87±5.39	5.26±4.64	12.565	<0.001
	D40	15.33±6.85	3.31±5.63	2.932	<0.001
	D20	25.02±9.35	9.57±12.99	11.955	<0.001
Left femoral heads	D _{max}	23.72±11.41	17.37±2.31	-2.389	0.030
	D _{mean}	8.11±3.73	5.83±4.02	-1.750	0.100
	D15	13.60±6.05	11.18±4.43	-1.067	0.303
	D5	17.11±7.88	14.05±2.68	-1.482	0.159
Right femoral heads	D _{max}	23.15±6.63	17.86±2.13	-3.432	0.004
	D _{mean}	7.28±3.09	6.46±3.73	-0.686	0.503
	D15	12.45±4.50	13.04±2.57	0.545	0.594
	D5	15.77±4.62	14.88±1.99	-0.855	0.406

Data are expressed as mean ± standard deviation ($\bar{x}\pm s$), and 2 is retained as a decimal. OARs, organs at risk; SBRT, stereotactic body radiotherapy; CIRT, carbon-ion radiation therapy; RBE, relative biological effectiveness.

a larger D_{max}.

Exposure dose of rectum

The D_{max} of SBRT and CIRT was 60.69±5.31 and 70.76±6.51 (P<0.001), D_{mean} was 13.87±5.39 and 5.26±4.64 (P<0.001), D40 was 15.33±6.85 and 3.31±5.63 (P<0.001), and D20 was 25.02±9.35 and 9.57±12.99 (P<0.001), respectively, all of which had significant differences. The relevant parameters are shown in *Table 4* and *Figure 4*. The rectum D_{max} of SBRT was lower, and the other exposure doses of CIRT were lower. The dose distribution was similar to that of the bladder.

Exposure dose of left/right femoral head

The left femoral head under SBRT and CIRT: D_{max} was 23.72±11.41 and 17.37±2.31 (P=0.03), D_{mean} was 8.11±3.73 and 5.83±4.02 (P=0.1), D15 was 13.60±6.05 and 11.18±4.43 (P=0.303), D5 was 17.11±7.88 and 14.05±2.68 (P=0.159), respectively; right femoral head: D_{max} was 23.15±6.63

and 17.86±2.13 (P=0.004), D_{mean} was 7.28±3.09 and 6.46±3.73 (P=0.503), D15 was 12.45±4.50 and 13.04±2.57 (P=0.594), D5 was 15.77±4.62 and 14.88±1.99 (P=0.406), respectively. The relevant parameters are shown in *Table 4* and *Figure 4*. The D_{max} of left/right femoral head of CIRT was significantly lower than that of SBRT; there was no significant difference in D_{mean}, D15, and D5, but the exposure dose of CIRT was lower, which had better protection for the femoral head.

Discussion

Prostate cancer is age-dependent to a certain extent. According to statistics, more than 85% of patients have an onset age of over 65 years. It is estimated that the proportion of elderly people over 65 years old in China will exceed 20% of the total population by 2040, and the incidence rate will increase gradually, so effective treatment method will benefit a large number of patients. There is

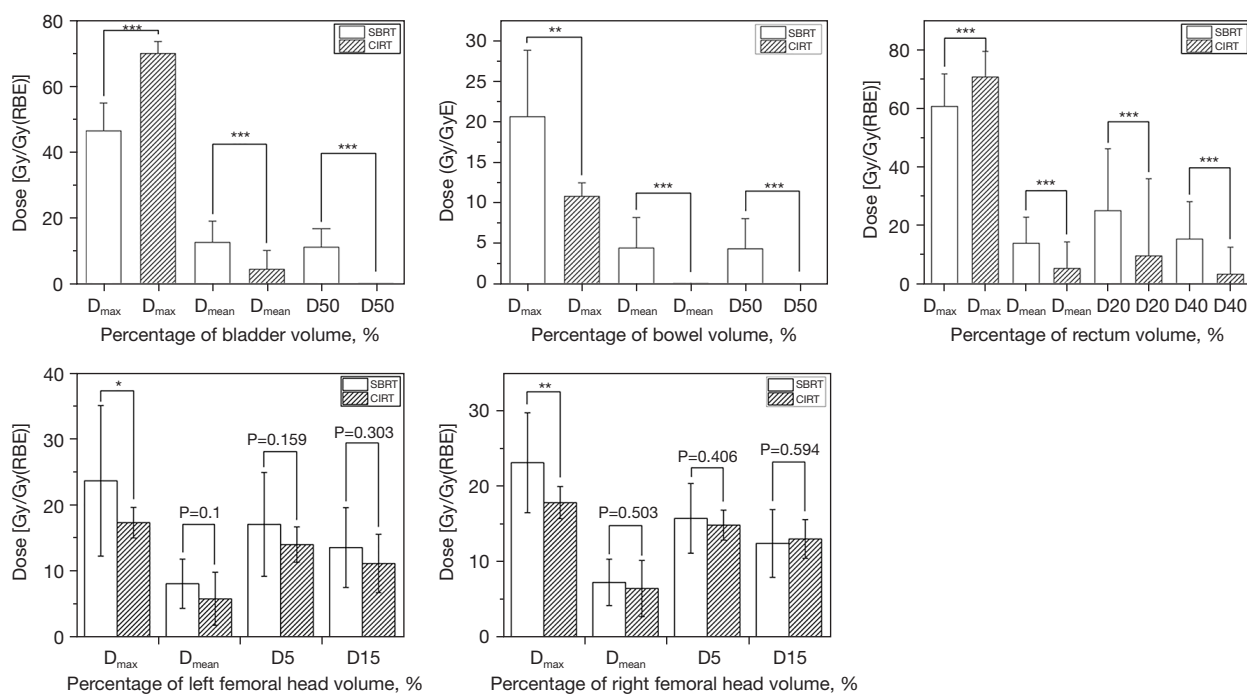


Figure 4 Volume dose histogram of OARs of 16 patients. *, $P < 0.05$; **, $P < 0.01$; ***, $P < 0.001$. D_{max} , maximum irradiation dose; D_{mean} , average irradiation dose; D50, minimum dose of 50% volume wrap; D20, minimum dose of 20% volume wrap; D40, minimum dose of 40% volume wrap; SBRT, stereotactic body radiotherapy; CIRT, carbon-ion radiation therapy; OARs, organs at risk.

a large difference in the α/β value between the tumor and surrounding OARs, and hence, there is a difference in radiation sensitivity, which makes it possible to perform hypo-fractionated radiotherapy (37).

In recent years, image-guided radiotherapy, precise planning, and precision radiotherapy treatment reflect the advances made in radiotherapy for prostate cancer (38,39). SBRT technology represented by CK has been widely used in clinical practice. High single dose, less fractions, accurate real-time target volume image tracking technology, and short treatment cycle improve the treatment comfort of patients and the quality of radiotherapy (40). Many research centers in China and abroad have shown that SBRT can achieve the same or better survival and curative effect in a shorter treatment course (41-44), which improves the quality of life of patients to a certain extent.

After nearly 30 years of clinical use, CIRT technology has gradually evolved. Compared to photon technology, it can significantly improve the overall survival (OS) and LC rate of the tumor, significantly reduce the toxicity and side effects on the gastrointestinal tract and achieve good curative effect (45-49). Its greatest advantage is reversed dose distribution and high biological effect. It changes the

$^{12}\text{C}^{6+}$ beam energy and adjusts the position of the Bragg peak to achieve high dose coverage of the tumor target volume, reduce the exposure to the surrounding normal tissues, and provide best protection for OARs. It is a novel radiotherapy method and has become a research hotspot in China and abroad in recent years, but further follow-up studies on a large number of cases is required to determine its clinical efficacy in China.

At present, both SBRT and CIRT are accurate radiotherapy technologies with several reports on their clinical efficacy, and their advantages have been confirmed. However, there are only a handful of reports on the dosimetric analysis of the same disease treated with these two technologies. In this study, we used the same BED, combined two different rays and different treatment methods, and further analyzed the advantages of SBRT and CIRT in individualized treatment from the perspective of dosimetry. In this study, however, after the optimization calculation of CK, 95% of the prescribed dose failed to cover 95% of the PTV volume as the primary foci of individual patients were surrounded by the intestine, or the primary foci were close to the rectum and bladder, or the volume of the primary focus was too large.

Dose distribution of target volume

Both treatment plans in this study fulfilled the clinical prescribed dose requirements and met the radiotherapy standards for prostate cancer. Under the same BED conditions, the average dose of SBRT target volume was higher, which may be related to the dose algorithm of CK to some extent. In the design of the treatment plan, 70% isodose line was required to cover at least 95% of the target volume, that is, 70% isodose line was the prescribed dose. Increasing this value can reduce the average exposure dose and improve the dose homogeneity of the target volume, but the dose may not meet the clinical treatment requirements, affecting the conformity of the target volume. At the same time, with the same BED, less fractions and higher single dose will lead to higher prescribed dose, resulting in an increase in the overall exposure dose.

The conformity of SBRT target volume was better, which may be related to the physical characteristics of CK itself. In this study, the CK radiation beams ranged from 300–496. The scattered beam made the dose concentrate mainly on the tumor target volume, and the dose gradient was steeper. However, CIRT had better coverage of the target volume and a more homogeneous dose distribution. The energy transfer value of $^{12}\text{C}^{6+}$ beam is a function of the incident depth. Most of the energy could be deposited at a specific tissue depth within a clear range, and the physical advantages of SOBP were fully reflected in the DVH diagram.

Dose distribution of OARs

Radiotherapy, however, inevitably causes radiation-related complications during treatment. Neal *et al.* (50) estimated that the influencing factors of the toxicity and side effects of radiotherapy on the rectum, bladder, and femoral head were 20, 5, and 1, respectively, but there are only a few reports on the toxicity and side effects on the femoral head and intestine (51). Therefore, it is necessary to reduce the exposure dose of the rectum and bladder during radiotherapy, and the dose value can affect the treatment effect to a certain extent.

From the perspective of the anatomical structure, the target volume is located between the bladder and rectum. Some patients had large foci that are close to the bladder and rectum, resulting in high-dose hotspots on the side close to the focus, thus making the D_{max} of CIRT significantly greater than CK. It has been reported that when the exposure dose of the bladder exceeds 60 Gy,

symptoms such as urgency of urination, hematuria, and cystitis may occur (52). In terms of D_{mean} and D_{50} , CIRT showed good physical characteristics, lower overall exposure dose, and better protection of bladder than CK. The dose distribution characteristics of the rectum were consistent with those of the bladder. It is important that the bladder is adequately full, and the rectum is emptied before radiotherapy. In this study, the maximum exposure doses of the bladder and rectum treated with CK were lower than 54.56 and 63.73 Gy (both converted to EQD₂) reported by Chatzikonstantinou *et al.* (53).

In terms of intestinal protection, except for two patients with partial target volume surrounded by the intestinal tract, which led to the D_{max} of CIRT being higher than that of CK, the D_{max} was lower for other patients. In this case, CK could disperse the dose, which was more advantageous for intestinal protection. However, the D_{mean} of CIRT was significantly lower than that of CK—it was basically close to 0 Gy (RBE) and better for intestinal protection.

For the left/right femoral head, the D_{max} of CIRT was significantly lower than that of CK, and there was no significant difference in the D_{mean} ; however, the dose of CIRT was lower, which may be related to the long distance of the femoral head from the target volume. In CIRT, the femoral head is located in the beam plateau region, which reduces the exposure dose. The CK beam has a hemispherical spatial distribution, so the overall exposure dose is higher than that of CIRT.

The RBE of carbon ions is complex and related to energy, LET value, tumor type, and therapeutic dose. In this study, we have only discussed the difference in dosimetric distribution of two different treatment plans at the same equivalent biological dose at the dosimetric level; we did not consider the influence of LET and RBE. This is also a limitation of this study. Another shortcoming of this study is that, due to the TPS system, the dose distribution map in CK cannot be displayed in the form of a cloud map, and the position of the sagittal bitmap also cannot be presented in the form of a mirror image, resulting in an inconsistency in the form of representation between the two. Due to the low incidence of prostate cancer in Gansu Province, we collected cases from several other units, and after screening for the two indications, the number of localized prostate cancer cases that were suitable for SBRT and CIRT treatment was not very large. Due to the limitation of the number of cases, we chose to conduct a holistic study and analyze all cases. We are considering separate studies for patients with different risk levels.

Conclusions

In this study, we found that both SBRT and CIRT met the clinical requirements of target volume and OARs in radiotherapy for localized prostate cancer. The PTV of prostate cancer under SBRT had better conformity and significantly higher dose in target volume, while the CIRT plan had higher coverage of target volume and more homogeneous dose distribution, and better protection for OARs, except for individual dose hotspots in the bladder and intestinal tract. Therefore, we recommend that the treatment techniques should be selected according to the local lesion volume and other specific conditions of low-, medium-, and high-risk patients with localized prostate cancer. In view of the limited number of cases included in this preliminary study, the results may be biased. Additionally, human factors can vary greatly among different clinicians. In future, studies with large clinical data are required to verify and support our conclusions.

Acknowledgments

Funding: This study was supported by the Infirmary Project of the 940th JLSF Hospital (No. 2022yxky019).

Footnote

Conflicts of Interest: All authors have completed the ICMJE uniform disclosure form (available at <https://qims.amegroups.com/article/view/10.21037/qims-23-340/coif>). The authors report that this study was supported by the Infirmary Project of the 940th JLSF Hospital (No. 2022yxky019). The authors have no other conflicts of interest to declare.

Ethical Statement: The authors are accountable for all aspects of the work in ensuring that questions related to the accuracy or integrity of any part of the work are appropriately investigated and resolved. This study was conducted in accordance with the Declaration of Helsinki (as revised in 2013). The study was approved by the Ethics Committee of the 940th Hospital of Joint Logistics Support Force of Chinese People's Liberation (No. 2022KYLL074). Written informed consent was obtained from all participants.

Open Access Statement: This is an Open Access article distributed in accordance with the Creative Commons

Attribution-NonCommercial-NoDerivs 4.0 International License (CC BY-NC-ND 4.0), which permits the non-commercial replication and distribution of the article with the strict proviso that no changes or edits are made and the original work is properly cited (including links to both the formal publication through the relevant DOI and the license). See: <https://creativecommons.org/licenses/by-nc-nd/4.0/>.

References

1. Carlsson SV, Vickers AJ. Screening for Prostate Cancer. *Med Clin North Am* 2020;104:1051-62.
2. Giri VN, Knudsen KE, Kelly WK, Cheng HH, Cooney KA, Cookson MS, et al. Implementation of Germline Testing for Prostate Cancer: Philadelphia Prostate Cancer Consensus Conference 2019. *J Clin Oncol* 2020;38:2798-811.
3. Van Poppel H, Albrecht T, Basu P, Hogenhout R, Collen S, Roobol M. Serum PSA-based early detection of prostate cancer in Europe and globally: past, present and future. *Nat Rev Urol* 2022;19:562-72.
4. Russo J, Giri VN. Germline testing and genetic counselling in prostate cancer. *Nat Rev Urol* 2022;19:331-43.
5. Bukavina L, Luckenbaugh AN, Hofman MS, Hope T, Kamran SC, Murphy DG, Yamoah K, Ost P. Incorporating Prostate-specific Membrane Antigen Positron Emission Tomography in Management Decisions for Men with Newly Diagnosed or Biochemically Recurrent Prostate Cancer. *Eur Urol* 2023;83:521-33.
6. Rasul S, Haug AR. Clinical Applications of PSMA PET Examination in Patients with Prostate Cancer. *Cancers (Basel)* 2022;14:3768.
7. Zheng R, Zeng H, Zhang S, Chen W. Estimates of cancer incidence and mortality in China, 2013. *Chin J Cancer* 2017;36:66.
8. Sung H, Ferlay J, Siegel RL, Laversanne M, Soerjomataram I, Jemal A, Bray F. Global Cancer Statistics 2020: GLOBOCAN Estimates of Incidence and Mortality Worldwide for 36 Cancers in 185 Countries. *CA Cancer J Clin* 2021;71:209-49.
9. Mohler JL, Antonarakis ES, Armstrong AJ, D'Amico AV, Davis BJ, Dorff T, et al. Prostate Cancer, Version 2.2019, NCCN Clinical Practice Guidelines in Oncology. *J Natl Compr Canc Netw* 2019;17:479-505.
10. Podder TK, Beaulieu L, Caldwell B, Cormack RA, Crass JB, Dicker AP, Fenster A, Fichtinger G, Meltsner MA, Moerland MA, Nath R, Rivard MJ, Salcudean T, Song DY, Thomadsen BR, Yu Y; American Association of Physicists

- in Medicine Brachytherapy Subcommittee and Therapy Physics Committee; Groupe Européen de Curiethérapie-European Society for Radiotherapy & Oncology BRAPHYQS Subcommittee. AAPM and GEC-ESTRO guidelines for image-guided robotic brachytherapy: report of Task Group 192. *Med Phys* 2014;41:101501.
11. Litwin MS, Tan HJ. The Diagnosis and Treatment of Prostate Cancer: A Review. *JAMA* 2017;317:2532-42.
 12. Cho LC, Timmerman R, Kavanagh B. Hypofractionated external-beam radiotherapy for prostate cancer. *Prostate Cancer* 2013;2013:103547.
 13. Onozawa M, Hinotsu S, Tsukamoto T, Oya M, Ogawa O, Kitamura T, Suzuki K, Naito S, Namiki M, Nishimura K, Hirao Y, Akaza H. Recent trends in the initial therapy for newly diagnosed prostate cancer in Japan. *Jpn J Clin Oncol* 2014;44:969-81.
 14. Pellegrino A, Cirulli GO, Mazzone E, Barletta F, Scuderi S, de Angelis M, Rosiello G, Gandaglia G, Montorsi F, Briganti A, Stabile A. Focal therapy for prostate cancer: what is really needed to move from investigational to valid therapeutic alternative?-a narrative review. *Ann Transl Med* 2022;10:755.
 15. Serra M, De Martino F, Savino F, D'Alesio V, Arrichiello C, Quarto M, Loffredo F, Di Franco R, Borzillo V, Muto M, Ametrano G, Muto P. SBRT for Localized Prostate Cancer: CyberKnife vs. VMAT-FFF, a Dosimetric Study. *Life (Basel)* 2022;12:711.
 16. Cheng Y, Lin Y, Long Y, Du L, Chen R, Hu T, Guo Q, Liao G, Huang J. Is the CyberKnife® radiosurgery system effective and safe for patients? An umbrella review of the evidence. *Future Oncol* 2022;18:1777-91.
 17. Gómez-Aparicio M, Valero J, Caballero B, García R, Hernando-Requejo O, Montero Á, Gómez-Iturriaga A, Zilli T, Ost P, López-Campos F, Couñago F. Extreme Hypofractionation with SBRT in Localized Prostate Cancer. *Curr Oncol* 2021;28:2933-49.
 18. Pompos A, Foote RL, Koong AC, Le QT, Mohan R, Paganetti H, Choy H. National Effort to Re-Establish Heavy Ion Cancer Therapy in the United States. *Front Oncol* 2022;12:880712.
 19. Li Y, Li X, Yang J, Wang S, Tang M, Xia J, Gao Y. Flourish of Proton and Carbon Ion Radiotherapy in China. *Front Oncol* 2022;12:819905.
 20. Chen RC. Radiation therapy for prostate cancer: An evolving treatment modality. *Urol Oncol* 2019;37:579-81.
 21. Hodapp N. The ICRU Report 83: prescribing, recording and reporting photon-beam intensity-modulated radiation therapy (IMRT). *Strahlenther Onkol* 2012;188:97-9.
 22. Salembier C, Villeirs G, De Bari B, Hoskin P, Pieters BR, Van Vulpen M, Khoo V, Henry A, Bossi A, De Meerleer G, Fonteyne V. ESTRO ACROP consensus guideline on CT- and MRI-based target volume delineation for primary radiation therapy of localized prostate cancer. *Radiother Oncol* 2018;127:49-61.
 23. Zhang Y, Li P, Yu Q, Wu S, Chen X, Zhang Q, Fu S. Preliminary exploration of clinical factors affecting acute toxicity and quality of life after carbon ion therapy for prostate cancer. *Radiat Oncol* 2019;14:94.
 24. Alongi F, Mazzola R, Fiorentino A, Corradini S, Aiello D, Figlia V, Gregucci F, Ballario R, Cavalleri S, Ruggieri R. Phase II study of accelerated Linac-based SBRT in five consecutive fractions for localized prostate cancer. *Strahlenther Onkol* 2019;195:113-20.
 25. Kulik C, Caudrelier JM, Vermandel M, Castelain B, Maouche S, Rousseau J. Conformal radiotherapy optimization with micromultileaf collimators: comparison with radiosurgery techniques. *Int J Radiat Oncol Biol Phys* 2002;53:1038-50.
 26. Mottet N, van den Bergh RCN, Briers E, Van den Broeck T, Cumberbatch MG, De Santis M, et al. EAU-EANM-ESTRO-ESUR-SIOG Guidelines on Prostate Cancer-2020 Update. Part 1: Screening, Diagnosis, and Local Treatment with Curative Intent. *Eur Urol* 2021;79:243-62.
 27. Michalski J, Lawton C, El Naqa I, Ritter M, O'Meara E, Seider M, Lee W, Rosenthal S, Pisansky T, Catton C, Valicenti R, Zietman A, Bosch W, Sandler H, Buyyounouski M, Ménard C. Development of RTOG consensus guidelines for the definition of the clinical target volume for postoperative conformal radiation therapy for prostate cancer. *Int J Radiat Oncol Biol Phys* 2010;76:361-8.
 28. Huang H. Dosimetric Study of Stereotactic Body Radiotherapy and Carbon Ion Radiotherapy for Prostate Cancer [D]; Lanzhou University, 2022.
 29. Gao X, Lu J, Li S, et al. Research on collimators on dose distribution and treatment time of Cyber Knife treatment planning. *Chinese Medical Equipment* 2015;12:39-42.
 30. Altundal Y, Cifter F, Mu G, Lee J, Wu EJ, Yeung V, Katz A. Prostate Stereotactic Body Radiation Therapy With Halcyon 2.0: Treatment Plans Comparison Based on RTOG 0938 Protocol. *Cureus* 2020;12:e11660.
 31. Ma X, Zhang Y, Zhang M, et al. Analysis of Dose Decay at the Edge of Beam in Heavy Ion Radiotherapy. *Journal of Oncology* 2021;27:390-4.
 32. Okada T, Tsuji H, Kamada T, Akakura K, Suzuki H,

- Shimazaki J, Tsujii H. Carbon ion radiotherapy in advanced hypofractionated regimens for prostate cancer: from 20 to 16 fractions. *Int J Radiat Oncol Biol Phys* 2012;84:968-72.
33. Brenner D, Martinez A, Edmundson G, Mitchell C, Thames H, Armour E. Direct evidence that prostate tumors show high sensitivity to fractionation (low alpha/beta ratio), similar to late-responding normal tissue. *Int J Radiat Oncol Biol Phys* 2002;52:6-13.
 34. Fowler J. The radiobiology of prostate cancer including new aspects of fractionated radiotherapy. *Acta Oncologica (Stockholm, Sweden)* 2005;44:265-76.
 35. Mesbahi A, Rasouli N, Mohammadzadeh M, Nasiri Motlagh B, Ozan Tekin H. Comparison of Radiobiological Models for Radiation Therapy Plans of Prostate Cancer: Three-dimensional Conformal versus Intensity Modulated Radiation Therapy. *J Biomed Phys Eng* 2019;9:267-78.
 36. Swanson E, Indelicato D, Louis D, Flampouri S, Li Z, Morris C, Paryani N, Slopsema R. Comparison of three-dimensional (3D) conformal proton radiotherapy (RT), 3D conformal photon RT, and intensity-modulated RT for retroperitoneal and intra-abdominal sarcomas. *Int J Radiat Oncol Biol Phys* 2012;83:1549-57.
 37. Kougioumtzopoulou A, Platoni K, Zygogianni A, Kounadis G, Syrigos KN, Psyri A, Bamias A, Kelekis N, Kouloulis V. Moderate Hypofractionated Radiotherapy for Localized Prostate Cancer: The Triumph of Radiobiology. *Rev Recent Clin Trials* 2021;16:351-71.
 38. Podder T, Song D, Showalter T, Beaulieu L. Advances in Radiotherapy for Prostate Cancer Treatment. *Prostate Cancer* 2016;2016:3079684.
 39. Podder TK, Fredman ET, Ellis RJ. Advances in Radiotherapy for Prostate Cancer Treatment. *Adv Exp Med Biol* 2018;1096:31-47.
 40. Coste-Manière E, Olender D, Kilby W, Schulz RA. Robotic whole body stereotactic radiosurgery: clinical advantages of the Cyberknife integrated system. *Int J Med Robot* 2005;1:28-39.
 41. Tree A, Ostler P, van der Voet H, Chu W, Loblaw A, Ford D, Tolan S, Jain S, Martin A, Staffurth J, Armstrong J, Camilleri P, Kancherla K, Frew J, Chan A, Dayes I, Duffton A, Brand D, Henderson D, Morrison K, Brown S, Pugh J, Burnett S, Mahmud M, Hinder V, Naismith O, Hall E, van As N. Intensity-modulated radiotherapy versus stereotactic body radiotherapy for prostate cancer (PACE-B): 2-year toxicity results from an open-label, randomised, phase 3, non-inferiority trial. *Lancet Oncol* 2022;23:1308-20.
 42. Parikh NR, Kishan AU. Stereotactic Body Radiotherapy for Prostate Cancer. *Am J Mens Health* 2020;14:1557988320927241.
 43. Kissel M, Créhange G, Graff P. Stereotactic Radiation Therapy versus Brachytherapy: Relative Strengths of Two Highly Efficient Options for the Treatment of Localized Prostate Cancer. *Cancers (Basel)* 2022;14:2226.
 44. Tsang YM, Tharmalingam H, Belessiotis-Richards K, Armstrong S, Ostler P, Hughes R, Alonzi R, Hoskin PJ. Ultra-hypofractionated radiotherapy for low- and intermediate risk prostate cancer: High-dose-rate brachytherapy vs stereotactic ablative radiotherapy. *Radiother Oncol* 2021;158:184-90.
 45. Chen X, Yu Q, Li P, Fu S. Landscape of Carbon Ion Radiotherapy in Prostate Cancer: Clinical Application and Translational Research. *Front Oncol* 2021;11:760752.
 46. Li P, Hong Z, Li Y, Fu S, Zhang Q. Two-Year Toxicity and Efficacy of Carbon Ion Radiotherapy in the Treatment of Localized Prostate Cancer: A Single-Centered Study. *Front Oncol* 2021;11:808216.
 47. Hiroshima Y, Ishikawa H, Iwai Y, Wakatsuki M, Utsumi T, Suzuki H, Akakura K, Harada M, Sakurai H, Ichikawa T, Tsuji H. Safety and Efficacy of Carbon-Ion Radiotherapy for Elderly Patients with High-Risk Prostate Cancer. *Cancers (Basel)* 2022;14:4015.
 48. Li M, Li X, Yao L, Han X, Yan W, Liu Y, Fu Y, Wang Y, Huang M, Zhang Q, Wang X, Yang K. Clinical Efficacy and Safety of Proton and Carbon Ion Radiotherapy for Prostate Cancer: A Systematic Review and Meta-Analysis. *Front Oncol* 2021;11:709530.
 49. Oike T, Sato H, Noda SE, Nakano T. Translational Research to Improve the Efficacy of Carbon Ion Radiotherapy: Experience of Gunma University. *Front Oncol* 2016;6:139.
 50. Neal AJ, Oldham M, Dearnaley DP. Comparison of treatment techniques for conformal radiotherapy of the prostate using dose-volume histograms and normal tissue complication probabilities. *Radiother Oncol* 1995;37:29-34.
 51. Abdulkareem I. Radiation-induced femoral head necrosis. *Niger J Clin Pract* 2013;16:123-6.
 52. Sun R, Koubaa I, Limkin EJ, Dumas I, Bentivegna E, Castanon E, Gouy S, Baratiny C, Monnot F, Maroun P, Ammari S, Zareski E, Balleyguier C, Deutsch É, Morice P, Haie-Meder C, Chargari C. Locally advanced cervical

- cancer with bladder invasion: clinical outcomes and predictive factors for vesicovaginal fistulae. *Oncotarget* 2018;9:9299-310.
53. Chatzikonstantinou G, Keller C, Scherf C, Bathen B,

Köhn J, Tselis N. Real-world dosimetric comparison between CyberKnife SBRT and HDR brachytherapy for the treatment of prostate cancer. *Brachytherapy* 2021;20:44-9.

Cite this article as: Huang HF, Gao XX, Li Q, Ma XY, Du LN, Sun PF, Li S. Dosimetric comparison between stereotactic body radiotherapy and carbon-ion radiation therapy for prostate cancer. *Quant Imaging Med Surg* 2023;13(10):6965-6978. doi: 10.21037/qims-23-340